Atmos. Meas. Tech. Discuss., 2, 3099–3127, 2009
www.atmos-meas-tech-discuss.net/2/3099/2009/

Atmospheric Measurement Techniques Discussions

This discussion paper is/has been under review for the journal Atmospheric Measurement Techniques (AMT). Please refer to the corresponding final paper in AMT if available.

A liquid nitrogen-free preconcentration unit for measurements of ambient N_2O isotopomers by QCLAS

J. Mohn, C. Guggenheim, B. Tuzson, M. K. Vollmer, and L. Emmenegger

Laboratory for Air Pollution & Environmental Technology, EMPA, Dübendorf, Switzerland

Received: 12 November 2009 – Accepted: 26 November 2009 – Published: 4 December 2009

Correspondence to: J. Mohn (joachim.mohn@empa.ch)

Published by Copernicus Publications on behalf of the European Geosciences Union.

Abstract

Important information about the biogeochemical cycle of nitrous oxide (N_2O) can be obtained by measuring its three main isotopomers, $^{14}N^{15}N^{16}O$, $^{15}N^{14}N^{16}O$, and $^{14}N^{14}N^{16}O$, and the respective site-specific isotope ratios $\delta^{15}N^{\alpha}$ and $\delta^{15}N^{\beta}$. Absorption laser spectroscopy in the mid-infrared is a direct method for N_2O isotopomer analysis, yet not sensitive enough for atmospheric N_2O concentrations (320 ppb). To enable a fully-automated high precision N_2O isotopomer analysis at ambient concentrations, we built and optimized a liquid nitrogen-free preconcentration unit to be coupled to a quantum cascade laser (QCL) based spectrometer. Rigorous tests were conducted, using FTIR and quantum cascade laser absorption spectroscopy (QCLAS), to investigate recovery rates, conservation of isotopic signatures and spectral interferences after preconcentration. We achieve quantitative N_2O recovery of >99% with only minor, statistically not significant isotopic fractionation and no relevant spectral interferences from other atmospheric constituents. The developed preconcentration unit also has the potential to be applied to other trace gases and their isotopic composition.

1 Introduction

Nitrous oxide (N_2O) is currently the most important anthropogenic ozone depleting substance and exerts the third largest greenhouse warming potential (Ravishankara et al., 2009). Since pre-industrial times, N_2O concentrations in the troposphere increased from 270 ppb (parts per billion, 10^{-9} molar) to the current level of 320 ppb at a rate of 0.26% yr^{-1}. The predominant sources of N_2O on a global scale are enhanced microbial production in expanding and fertilized agricultural lands, as well as biomass and fossil fuel burning. While the major sink, stratospheric destruction, is well quantified, the strengths of N_2O sources remain largely uncertain (Solomon et al., 2007).

Important information about the biogeochemical cycle of N_2O can be obtained by measuring the intramolecular distribution of ^{15}N in atmospheric N_2O (Billings, 2008;

AMTD

2, 3099–3127, 2009

Bernard et al., 2006; Ishijima et al., 2007; Rahn and Wahlen, 2000; Röckmann et al., 2003; Röckmann and Levin, 2005; Yoshida and Toyoda, 2000). N_2O is a linear three-atom molecule with one nitrogen atom in the centre (2 or α site) and one at the end (1 or β site) which has four possible stable isotopic species with respect to nitrogen isotopes. The most abundant N_2O isotopic species in the atmosphere are $^{14}N^{14}N^{16}O$ (99%), $^{15}N^{14}N^{16}O$ (0.37%) and $^{14}N^{15}N^{16}O$ (0.37%) (Werner and Brand, 2001; Yoshida and Toyoda, 2000). Isotope abundances are usually reported in the δ-notation, where $\delta^{15}N$ denotes the relative difference in ‰ of the $^{15}N/^{14}N$ ratio of the sample versus the reference material (atmospheric N_2), analogically $\delta^{15}N^{\beta}$ denotes the corresponding ratio for $^{15}N^{14}N^{16}O$ vs. $^{14}N^{14}N^{16}O$.

The bulk nitrogen isotope ratio ($\delta^{15}N^{bulk} = (\delta^{15}N^{\alpha} + \delta^{15}N^{\beta})/2$) of tropospheric N_2O is enriched by approximately 7.0‰ relative to air-N_2, with a strong site preference (SP=$\delta^{15}N^{\alpha} - \delta^{15}N^{\beta}$) of 18.7‰ for the central nitrogen atom (Yoshida and Toyoda, 2000). Tropospheric N_2O concentrations and isotopic composition are largely controlled by back injection of stratospheric N_2O as well as N_2O emissions from microbial activity and combustion processes. In the stratosphere, the abundance of the heavier isotopomers and the SP increases with altitude to values as high as 100‰ at 35 km, mainly due to isotopic fractionation during UV-induced photolysis and oxidation, while the N_2O mixing ratio decreases to 10–20 ppb (Toyoda et al., 2001). Isotopomer ratios of different N_2O emission sources were found to vary largely between approx. −50‰ (soil) to 10‰ (coal combustion) for $\delta^{15}N^{bulk}$ and −5‰ (soil) to 35‰ (ocean) for the SP (Toyoda et al., 2009, and references therein). The required analytical precision for $\delta^{15}N^{\alpha}$ and $\delta^{15}N^{\beta}$ depends strongly on the application and may vary between <0.1‰ for firn air analysis to 1‰ for subsoil N_2O studies.

Currently, the only technique for N_2O isotopic measurements at ambient concentrations is laboratory-based isotope-ratio mass-spectrometry (IRMS) in combination with flask-sampling. However, isotopomers such as $^{14}N^{15}N^{16}O$ and $^{15}N^{14}N^{16}O$ cannot be distinguished directly by IRMS, as they have the same mass. To determine the site-selective isotopic composition, the ^{15}N content of the NO^+ and N_2O^+ ions has to be

AMTD
2, 3099–3127, 2009

analyzed (Brenninkmeijer and Röckmann, 1999; Toyoda and Yoshida, 1999). Therefore, the masses *m/z* 44, 45, and 46 (for N_2O) and *m/z* 30 and 31 (for NO) are monitored either simultaneously (on last generation IRMS) or after two separate sample injections. Although IRMS is a well-known method with excellent precision (0.05‰–0.9‰) and accuracy (Röckmann and Levin, 2005; Well et al., 2008; Yoshida and Toyoda, 2000), it has some disadvantages such as the large size of the instrument, which hinders field measurements. The required field sampling and sample storage strongly limits its use for the characterization of variations in N_2O isotopic species at time-scales relevant to many environmental processes.

Laser spectroscopy is a valuable alternative, because compact and continuously-operating instruments can be developed that allow for extended field measurements. This offers the possibility for process studies and opens a completely new field of applications. Furthermore, the method is inherently selective, even for molecules with the same mass, because it is based on the highly characteristic rotational-vibrational transitions of the different N_2O isotopomers. The absorption lines of the various species can be easily resolved at low cell pressure. However, there are only a few spectroscopic measurements on isotope ratios of N_2O, and these were performed on pure N_2O samples (Gagliardi et al., 2005; Nakayama et al., 2007; Uehara et al., 2001, 2003) with the exception of two recent studies (Wächter et al., 2008; Wächter and Sigrist, 2007). The reported precisions range between 0.2‰ and 9‰.

Recent advances in laser technology provided a new class of mid-infrared (IR) semiconductor lasers: the unipolar intersubband quantum cascade lasers (QCL). They have the advantage of operating at non-cryogenic temperatures (quasi room-temperature) with high spectral purity and relatively high power output (Faist et al., 1994). The application of these light sources for high-precision isotope ratio measurement has been recently demonstrated for CO_2 by Nelson et al. (2008) and Tuzson et al. (2008a, b). Spectroscopy in the mid-IR region is particularly effective for molecules that exhibit strong fundamental vibrations, such as CO_2 and N_2O, with line intensities about two orders of magnitude higher than in the near-IR. We recently demonstrated a precision

AMTD
2, 3099–3127, 2009

of 0.5‰ for δ^{15}N at N_2O concentrations of 90 ppm (Wächter et al., 2008) using a pulsed QCL emitting at 4.6 μm (Alpes Lasers, Switzerland). Atmospheric N_2O concentrations (320 ppb), however, are more than two orders of magnitude lower and are therefore currently not accessible for direct isotopic analysis by laser spectroscopy.

For these reasons we suggest to combine laser spectroscopy with preconcentration techniques to increase N_2O concentrations from ambient levels to ~60 ppm. The developed custom-built preconcentration unit enables us to make use of the precision and site specificity of QCLAS at a temporal resolution of approx. 30 min. The preconcentration technique we employ is fully automated and is based on a commercial closed-loop cryogenic unit and thereby free of consumables like liquid nitrogen. Here we describe the most important properties that were obtained through systematic optimization and characterization: (a) excellent recovery of N_2O and other trace gases; (b) conservation of the N_2O isotope ratios, and (c) negligible impact of other atmospheric constituents (e.g. CO_2, H_2O, CO, O_3, CH_4 and C_2H_2) on the analyzed N_2O isotopomer ratios. Our results also indicate that the coupling of preconcentration and laser spectroscopy may be feasible for other trace gases and their isotopes (e.g. many VOCs, CH_4, CO).

2 Experimental

2.1 Instrumental

2.1.1 Preconcentration unit

The technology of our preconcentration unit is based on a previously developed system called “Medusa” which was originally designed for halogenated compounds measurements by gas-chromatography mass-spectrometry (Miller et al., 2008). We re-designed and optimized the system for the preconcentration of N_2O isotopomers and their subsequent quantification by laser spectroscopy. One main reason to choose this system is the combination of a relatively mild adsorbent trap with a low-temperature refrigeration

AMTD
2, 3099–3127, 2009

unit reaching <−150°C. Our preconcentration unit differs from "Medusa" by the followings: a simplified setup with two instead of five valves and one instead of two adsorbent traps. Furthermore, all gas flows are regulated by mass flow controllers (MFC, Redy Smart Series, Vögtlin Instruments, Switzerland) and the complete preconcentration unit is controlled and monitored by LabVIEW (National Instruments Corp., USA) programming.

The instrument flow scheme is illustrated in Fig. 1, showing one particular position of the valves (Valco Instruments Inc, Switzerland), which are used to isolate or combine various sections of the sample pathways. The 6-port valve is equipped with an elongated-groove rotor and driven by a multi-position actuator which enables more than 2 valve positions. Rotating the 4-port valve will change the flow direction through the HayeSep D trap. The preconcentration trap consists of stainless steel tubing (ID 1.6 mm, OD 2.1 mm) filled with 200 mg HayeSep D (100–120 mesh, Hayes Separations Inc., USA) and coiled onto an aluminium tube standoff. The standoff is attached to a copper base-plate cooled by the refrigeration unit (PCC: Polycold Compact Cooler, Brooks Automation, USA), and located in a vacuum chamber. The trap reaches temperatures of ∼−150°C and can be heated resistively to >100°C, using a custom-built trap heating unit coupled with an Omega PID controller (CN77354-C2, Omega Engineering Inc., USA).

The operation sequence and parameter settings (e.g. flow rates, temperatures and timing) of the preconcentration unit were optimized to obtain a sharp N_2O concentration profile during desorption. The principle of operation is described in the following paragraphs (see Figs. 1 and 2).

After an initialization phase that sets all parameters to their starting values, the HayeSep D trap is purged by back-flushing with 50 sccm (standard cubic centimetre per minute) of high purity synthetic air (79.5% N_2, 20.5% O_2) and heated to approx. −50°C (phase I). This phase assures the absence of residual N_2O on the preconcentration trap and reproducible starting conditions but may be omitted during continuous operation to improve the temporal resolution. After cooling the trap down to ∼−150°C, the loading

(phase II) is initialized by setting the sample gas flow to 500 sccm, flushing the lines and rotating the 6-port valve to the loading position. H_2O and CO_2 are removed from the measuring gas by a Nafion^{TM} drier (MD-050-72S-1, PermaPure Inc., USA) and a chemical trap filled with Ascarite (3 g, 10–35 mesh, Fluka, Switzerland) bracketed by $Mg(ClO_4)_2$ (2×3 g, Fluka, Switzerland). To purge residual gas molecules onto the trap, a short post-flush with synthetic air is applied at the end of phase II. Rotating the 4-port valve to position 2 (backward flow) and adjusting the flow of synthetic air to 50 sccm initiates the desorption (phase III). After setting the trap temperature to −50°C, an immediate release of N_2O can be observed by FTIR spectroscopy (see Fig. 2). Finally, all parameters and conditions are set back to their initial values.The duration of trap loading (phase II) and desorption (phase III) are adjusted based on the desired/available sample volume (standard procedure: 20 min at 500 sccm sampling flow results in 10 l sample volume) and the desired N_2O output concentration, usually around 60 ppm for high precision N_2O isotopomer analysis by QCLAS. The minimal desorption time for quantitative N_2O recovery depends on the molar N_2O input and was determined by on-line FTIR spectroscopy to be between 60 s for 140 nmol and 180 s for 4000 nmol N_2O. Typically a 10 l ambient air sample is focused into 50 ml desorption volume, corresponding to a concentration factor of 200.

2.1.2 On-line FTIR concentration measurement

We employed a Nicolet Avatar 370 MCT spectrometer (Thermo Nicolet Corp., USA) equipped with a heated (40°C) low-volume (50 ml) flow-through gas cell with 1 m pathlength (Model LFT-210, Axiom Analytical Inc., USA). An infrared spectrum with 0.5 cm^{-1} optical resolution was recorded every three seconds, and trace gas (N_2O, CO, CH_4, CO_2 and H_2O) concentrations were retrieved by classical least square fitting in selected wavelength regions (Mohn et al., 2004; Mohn et al., 2008). Calibration spectra were recorded under identical instrumental and spectroscopic conditions from certified and diluted calibration gases or by continuous injection of liquids into nitrogen. The detection limits (VDI, 1995) for the trace gases in the undiluted gas were: 100 ppb

N_2O, 200 ppb CH_4, 1 ppm CO_2, 200 ppb CO, 10 ppm H_2O. The expanded standard uncertainty for these components is around 10% (95% confidence level). The response time (t_{95}) for the experimental setup (sampling line, FTIR gas cell) was 55 s at the applied flow rate of 50 sccm and 13 s employing a fed-in flow of 450 sccm synthetic air in front of the gas cell to determine the minimal desorption time of the preconcentration unit.

2.1.3 Analysis of N_2O isotopomers by QCLAS

The QCL based spectrometer used in the present project is an improved version of the instrument used by Wächter et al. (2008). The experimental setup consists of a single-mode, pulsed quantum cascade laser emitting at 4.6 μm, a multipass absorption cell (optical path length 56 m, volume 500 ml; Aerodyne Research Inc., USA) and a detection system with pulse normalization. Laser control, data acquisition and real-time signal processing are performed by the TDLWintel software (Aerodyne Research Inc., USA). The main updates include: (a) a new RT-QCL (Alpes Lasers SA, Switzerland) with about 10 times more power and a considerably narrower line width of 0.0068 cm^{-1}; (b) a new generation thermo-electrically cooled detector (PVI-3TE-5, Vigo System, PL) with a specific detectivity (D*) $>10^{11}$ at 4.5–4.6 μm, coupled to a miniaturized preamplifier and TEC-controller (MTCC-01, Vigo System, PL). The detector assembly is mounted on a water-cooled cold-plate, which maintains a stable heat-sink temperature of 15±0.1°C. Further improvements were achieved by redesigning the laser current and temperature control unit, optimizing the laser pulser electronics and the 3-D-alignment stage of the collimating optics for a better alignment stability.

The selected absorption lines for this study are shown in Fig. 3. They are located within the scanning range of the laser and have sufficiently strong line strength with similar absorbance for each isotopic species. Mixing ratios for the different species are obtained by simultaneously fitting a low-order polynomial to the spectral baseline and a Gaussian-convoluted Voigt profile to the observed absorption lines, taking into account the measured path length, gas temperature (~307 K), pressure (8 kPa) and laser line

width. For the site-specific isotope ratios $\delta^{15}N^{\alpha}$ and $\delta^{15}N^{\beta}$, a precision of 0.2–0.3‰ was obtained at 90 ppm N_2O using the Allan variance approach (Werle et al., 1993, data not shown). N_2O concentration measurements (Sect. 2.2.1) were performed at 2188.19 cm^{-1}. The QCL spectrometer was operated with a continuous input gas flow of 50–70 sccm.

2.2 Validation of N_2O preconcentration unit

To validate the N_2O preconcentration unit, tests were performed on the quantitative recovery of N_2O and other trace gases (Sect. 2.2.1), on the conservation of the N_2O isotope ratios ($\Delta\delta^{15}N=\delta^{15}N_{precon}-\delta^{15}N_{original}$) (Sect. 2.2.2), and on the composition of preconcentrated ambient air and its potential interferences with N_2O isotopic analysis (Sect. 2.2.3).

To investigate the trace gas recoveries and isotopic fractionation effects, gas mixtures with known concentrations and/or isotopic composition were prepared from standard reference gases by dynamic dilution with synthetic air ($N_2O<0.3$ ppb) and/or pressurized air using a pair of MFCs. Standard reference gases applied include 9.0 ppm and 90 ppm N_2O in synthetic air (Messer Schweiz, Switzerland) to determine the trace gas recoveries and gravimetrically prepared 90.8 ppm N_2O in synthetic air with known isotopic composition ($\delta^{15}N^{\alpha} = \delta^{15}N^{\beta}$=25.4‰ versus medical grade N_2O) to investigate the conservation of the N_2O isotope ratios (Wächter et al., 2008). Table 1 summarizes the gas mixtures used during the various validation experiments. For the study of spectral interference we relied on ambient air sampled with a membrane pump (PTFE coated membrane, N 035 AT.18, KNF Neuberger, Switzerland).

2.2.1 Trace gas recovery

For the determination of the trace gas recovery, 1 to 10 l of a gas mixture were supplied at a flow rate of 100 sccm, containing N_2O, CH_4 and CO at ambient concentrations and H_2O and CO_2 at sub-ambient concentrations (Table 1). While these tests were based on the standard preconcentration procedure, no chemical trap was employed to investigate the influence of H_2O and CO_2 traces on the N_2O adsorption. On-line FTIR measurements were performed to obtain time-resolved information on the trace gas concentrations desorbed from the HayeSep D trap. The molar amount of desorbed trace gases were calculated as the integrals over time of the output trace gas concentrations and the flow rates of synthetic air applied for desorption. The chosen approach has the advantage of analyzing the recovery for different trace gases under standard operation conditions but does not allow a highly precise budgeting because it relies on a fast integration over a wide concentration range and on MFCs and gas flows that are different during adsorption and desorption.

To achieve an even better precision for the determination of the N_2O recovery, a second approach was used. These further experiments were designed to yield the same concentration before and after the preconcentration step due to the use of the same MFC (MFC2) and flow parameters (2400 s and 100 sccm) during adsorption and desorption, and by collecting the desorbed sample in a 10 l Tedlar bag (Product No. 245-08, SKC Inc., USA). The sample gas was dynamically diluted from a tank, containing either 9.0 or 90 ppm N_2O in synthetic air, with synthetic air to ambient (350 ppb), intermediate (900 ppb) or process (9.0 ppm) concentrations (Table 1). N_2O concentrations in the sample gas and in the desorbed sample (Tedlar bag) were compared based on QCLAS at 2188.19 cm^{-1}. Experiments at every concentration were replicated thrice. Small differences (<1%) between the adsorbed and desorbed gas volumes, as recorded by LabVIEW from the MFC output, were corrected.

AMTD
2, 3099–3127, 2009

2.2.2 Isotopic fractionation

To validate the conservation of isotopic signatures, a N_2O reference gas (90.8 ppm N_2O) with known isotopic composition ($\delta^{15}N^{\alpha} = \delta^{15}N^{\beta}$=25.4‰ versus medical grade N_2O) was diluted using high-purity synthetic air prior to preconcentration, followed by Tedlar bag sampling and QCLAS analysis (Table 1). Ambient (350 ppb), intermediate (900 ppb) and process (9.0 ppm) N_2O concentrations were deployed for preconcentration. The standard preconcentration procedure was applied with an adsorption flow rate of 500 sccm during 20 min and 50 sccm (60–150 s) desorption flow. At elevated N_2O input concentrations (9.0 ppm) the desorbed sample gas was dynamically diluted by 1:10 during desorption as a fed-in flow, resulting in concentrations of ~60 ppm for all experiments. A series (n=5–70) of preconcentration cycles were pooled in one Tedlar bag to obtain a gas sample of 3 to 5 l. Experiments at every concentration were replicated three to five times.

The N_2O isotopic composition of these samples after preconcentration was compared to the same reference gas diluted with synthetic air to a comparable N_2O concentration (±1 ppm) to calculate $\Delta\delta^{15}N = \delta^{15}N_{precon} - \delta^{15}N_{original}$. All measurements ($n$=4–8) were done on a relative scale using medical grade N_2O (91.1 ppm N_2O) which we define as $\delta^{15}N^{\alpha} = \delta^{15}N^{\beta}$=0‰ and a gravimetrically prepared enriched gas (90.8 ppm N_2O, $\delta^{15}N^{\alpha} = \delta^{15}N^{\beta}$=25.4‰ versus medical grade N_2O) for calibration (Wächter et al., 2008).

2.2.3 Spectral interference

To evaluate potential spectral interferences from ambient air, samples were taken through a 5 m, 6 mm outer diameter PTFE tube from outside the laboratory building. The corresponding trace gas concentration values were taken from the routine measurements at the ~300 m distant station Dübendorf of the Swiss National Air Pollution Monitoring Network (NABEL). Where no NABEL data were available (N_2O

and CO_2), we assumed typical ambient concentrations as shown in Table 1. The standard preconcentration procedure (Sect. 2.1.1) was followed, and the desorbed gaseous species were analyzed either continuously (O_3, N_2O, CO_2, H_2O, CH_4, CO) or after Tedlar bag sampling (C_2H_2, O_2). Continuous data after preconcentration were obtained by FTIR (Sect. 2.1.2) for N_2O, CO_2, H_2O, CH_4, and CO. Ozone was measured using an UV absorption O_3 analyzer (TEI 49C, Thermo Fisher Scientific Inc., USA) after dynamic dilution with synthetic air. Oxygen was determined with an O_2 analyzer (Servomex 570A, Spectris plc, UK), and acetylene concentrations were obtained using a GC-FID (Agilent 6890 with Plot Al_2O_3 (KCl) column) after preconcentration with a Peltier cooled HayeSep D trap. The concentrations and corresponding preconcentration factors were then used to simulate absorption spectra and evaluate possible spectral interferences.

3 Results and discussion

3.1 Trace gas recovery

Quantitative recovery of the adsorbed trace gases is a prerequisite to assure the representativeness of the analyzed gas sample and to avoid fractionation effects. Two different approaches were chosen to tackle this subject: (i) determination of the trace gas recovery with increasing adsorption volume to examine the trap capacity (Fig. 4); (ii) high-precision recovery of N_2O at different concentration levels (Table 2).

The capacity of the adsorbent trap for different trace gases was evaluated based on a sequence of experiments where 1 to 10 l of a gas mixture with constant composition (see Table 1) were first adsorbed on the preconcentration trap and then desorbed with a flow of 50 sccm of synthetic air and analyzed by on-line FTIR spectroscopy. For every trace gas the molar amounts in the input and output gas volume were calculated, integrating over time the respective concentrations and gas flows.

AMTD
2, 3099–3127, 2009

The CO concentration in the output flow was below the FTIR detection limit of 200 ppb and the amount of desorbed CH_4 was nearly constant and did not depend on gas sample volume (Fig. 4). This indicates that the mild adsorbent HayeSep D does not quantitatively retain CH_4 and CO at a trap temperature of approx. −150°C which is above their respective boiling points of −161°C and −191.5°C.

For high precision N_2O isotopomer analysis by QCLAS the loss of CO is an advantage because of its absorption in the selected spectral region. The application of the preconcentration unit for CO and CH_4 may still be envisaged by employing a stronger adsorbent (i.e. Molsieve 5Å) or an alternative refrigerant reaching a lower adsorption temperature.

As shown in Fig. 4, for N_2O and CO_2 a linear relation in the molar amounts between the trap output and the sample volumes was obtained, with expanded standard uncertainties for the regression lines of less than 1%. The linearity holds for the full investigated range, while the slight deviation from unity of 2% to 6%, is well below the uncertainty due to potential systematic offsets in the input and output gas concentration measurements by FTIR or in the input and output gas flows.

The efficiency of N_2O recovery is critical, because the adsorption/desorption processes may lead to significant isotopic fractionation (Bertolini et al., 2005; Brand, 1995; Werner et al., 2001). Therefore, a second, more precise approach was applied which allows the direct comparison of the sample gas before and after preconcentration by precise QCLAS measurements (Sect. 2.2.1). Using this experimental setup, the input and output concentrations agreed within 0.2% at ambient (350 ppb), intermediate (900 ppb) and process levels (9.0 ppm) (Table 2). Apart from the standard deviation for repetitive measurements, systematic deviations from e.g. subtle differences between the adsorbed and desorbed gas volumes cannot be excluded. However, such effects are considerably smaller than 1%, corresponding to a >99% recovery and thus, we expect only minimal, if any, isotopic fractionation.

3.2 Isotopic fractionation

To further confirm the conservation of isotopic signatures the isotopic composition of samples at ambient (350 ppb), intermediate (900 ppb) or process concentrations (9 ppm) were compared before and after preconcentration as described in Sect. 2.2.2. All experiments were done with gases that were enriched in $\delta^{15}N^{\alpha}$ and $\delta^{15}N^{\beta}$ at a level of 25.4‰.

Agreement of the N_2O isotopic composition with/without preconcentration was in general very good (see Table 3). The $\delta^{15}N^{\alpha}$ isotope ratio of N_2O after preconcentration are within 0.1‰ with the unprocessed calibration gas. For $\delta^{15}N^{\beta}$, the data seems to indicate a slight increase in the $\delta^{15}N^{\beta}$ values after preconcentration, particularly at lower N_2O input concentrations. The uncertainty of the mean values is however rather large, and in a one-sided student's t-test the effect is not significant at the 0.05 significance level. We, nevertheless, plan to repeat the experiments in the future with the next generation of QCLAS and a directly coupled preconcentration unit. It should also be noted that the calibration routine will include the preconcentration step and can thus be expected to largely account for small fractionation effects if they really occur.

3.3 Spectral interference

At the precision levels needed for N_2O isotope ratio analysis, even very weak spectral interferences of other compounds may be detrimental. To analyze spectral interferences of ambient air constituents the following approach was applied: (i) identification of molecular species (based on HITRAN database) that may cause spectral interferences through their absorption features; (ii) quantitative analysis of these components after preconcentration of ambient air, and (iii) assessment of spectral interferences based on spectral simulations.

Although the chosen absorption lines are free of any strong or obvious interferences, we have considered all molecules in the HITRAN database (Rothman et al., 2005) for lines in the relevant wavelength region. The line strengths of the relevant molecules are

AMTD
2, 3099–3127, 2009

plotted in Fig. 5(b), weighted for their ambient molecular abundance (Table 1). Based on this abundance weighted representation, the most relevant interfering compounds are H_2O and CO_2, followed by CO, O_3 and C_2H_2. Apart from its spectral interference, the water content in the measuring gas has to be reduced considerably to avoid clogging of the adsorption trap. This is accomplished by permeation drying and $Mg(ClO_4)_2$, while CO_2 is largely removed by the Ascarite trap. For the other gas compounds, the preconcentration procedure is quite selective, as will be shown below.

Concentrations of H_2O and CO_2 were efficiently reduced during preconcentration, below their FTIR detection limits of 10 and 1 ppm, respectively. Both H_2O and CO_2 were shown to be efficiently removed by chemical trapping with $Mg(ClO_4)_2$ and Ascarite to ppm or even ppb levels, respectively (Röckmann and Levin, 2005; Mohn et al., 2007). The average ozone output concentration was only about six times the ambient concentration which corresponds to a 3% recovery, assuming a concentration factor of 200. This can be expected because ozone is subject to rapid decomposition during desorption at hot metal surfaces. CH_4 and CO are not efficiently trapped by the preconcentration unit, due to their low boiling points, as reflected by a breakthrough of >98%. The C_2H_2 output concentration was around 125 ppb, which would correspond to an input concentration of 0.62 ppb assuming a quantitative recovery. This value is in-between the annual average C_2H_2 concentrations observed at the remote NABEL-station Rigi-Seebodenalp and the urban station Zurich with 0.4 and 1.0 ppb (FOEN and EMPA, 2009), respectively, which is in accordance with the suburban character of the sampling station Dübendorf.

O_2 and N_2 are to a large extent lost during trapping. The remaining bulk gases increased the O_2/N_2 ratio by 2–3% in the synthetic air employed for desorption, most probably due to the larger N_2 loss during trapping as a result of the difference in boiling points of −183.0°C and −195.8°C of O_2 and N_2, respectively. This slight change in the gas matrix should, however, not have any significant effect on the isotope ratio measurements since the reference gases will also be supplied in synthetic air and treated similarly.

A hypothetical absorption spectrum was generated, based on the analyzed output concentrations and typical conditions employed for QCLAS measurements (Sect. 2.1.3). To obtain a meaningful representation, the spectrum of preconcentrated ambient air was multiplied by a factor of 1000 (Fig. 5), reflecting the required precision for the N_2O isotopomer ratios in the sub-per mille range. The only relevant signals might be due to very weak O_3, CO and C_2H_2 absorption. The resulting effect on the isotopomer concentrations is, however, below 1% (even with a 1000× magnification) in a typical retrieval of concentrations from measured spectra, which translates into a shift of less than 0.01‰ on the δ-scale.

4 Conclusions

We built, optimized and validated a liquid nitrogen-free fully-automated preconcentration unit to increase N_2O concentrations by a factor of 200 from ambient levels to about 60 ppm. The key element is the combination of a relatively mild adsorbent with a low temperature refrigeration unit, achieving trapping temperatures of approximately −150°C. During standard operation, 140 nmol of N_2O are adsorbed from 10 l of ambient air within 20 min and desorbed in 50 ml of high purity synthetic air. The validation experiments showed quantitative N_2O recovery with only minor, statistically not significant isotopic fractionation, and negligible spectroscopic interferences from other atmospheric constituents on the analyzed N_2O isotopomer ratios.

Based on these encouraging results we intend to directly couple the preconcentration unit to a QCL spectrometer to permit fully-automated high precision (<0.5‰ for $\delta^{15}N$) N_2O isotopomer analysis at ambient concentrations (~320 ppb) with a temporal resolution of less than 30 min. Expected spectroscopic improvements, e.g. using continuous lasers and/or spectral ratio methods will provide enhanced precision without significant modifications in the instrumental setup. Future modifications of this basic setup may permit to analyze other trace gases that are not directly accessible by currently available spectroscopic techniques (i.e. many VOCs) and to quantify isotopologues of

substances at relatively low concentrations, such as CH_4, CO and organic compounds by employing a stronger adsorbent (i.e. Molsieve 5Å) or an alternative refrigerant reaching a lower adsorption temperature.

Acknowledgements. We acknowledge the support of Matthias Hill, Angelina Wenger and Benjamin R. Miller for the construction of the preconcentration unit, based on their extensive knowledge of the original "Medusa" for GC-MS. Wilhelm Gutjahr helped to conduct the numerous experiments needed to optimize the experimental conditions. Davide Ferri provided the FTIR gas cell, and Erwin Pieper and Willy Knecht contributed with their competence in mechanical design and electronics.

References

Bernard, S., Röckmann, T., Kaiser, J., Barnola, J.-M., Fischer, H., Blunier, T., and Chappellaz, J.: Constraints on N_2O budget changes since pre-industrial time from new firn air and ice core isotope measurements, Atmos. Chem. Phys., 6, 493–503, 2006, http://www.atmos-chem-phys.net/6/493/2006/.

Bertolini, T., Rubino, M., Lubritto, C., D'Onofrio, A., Marzaioli, F., Passariello, I., and Terrasi, F.: Optimized sample preparation for isotopic analyses of CO_2 in air: Systematic study of precision and accuracy dependence on driving variables during CO_2 purification process, J. Mass Spectrom., 40, 1104–1108, doi:10.1002/jms.888, 2005.

Billings, S. A.: Biogeochemistry: Nitrous oxide in flux, Nature, 456, 888–889, doi:10.1038/456888a, 2008.

Brand, W. A.: PRECON: A fully automated interface for the pre-GC concentration of trace gases in air for isotopic analysis, Isot. Environ. Healt. S., 31, 277–284, doi:10.1080/10256019508036271, 1995.

Brenninkmeijer, C. A. M. and Röckmann, T.: Mass spectrometry of the intramolecular nitrogen isotope distribution of environmental nitrous oxide using fragment-ion analysis, Rapid Commun. Mass Sp., 13, 2028–2033, doi:0951-4198/99/202028-06, 1999.

Faist, J., Capasso, F., Sivco, D. L., Sirtori, C., Hutchinson, A. L., and Cho, A. Y.: Quantum Cascade Laser, Science, 264, 553–556, doi:10.1126/science.264.5158.553, 1994.

FOEN and EMPA: Luftbelastung 2008, Messresultate des Nationalen Beobachtungsnetzes für Luftfremdstoffe (NABEL), Bern, 139 pp. , 2009.

Gagliardi, G., Borri, S., Tamassia, F., Capasso, F., Gmachl, C., Sivco, D. L., Baillargeon, J. N., Hutchinson, A. L., and Cho, A. Y.: A frequency-modulated quantum-cascade laser for spectroscopy of CH_4 and N_2O isotopomers, Isot. Environ. Healt. S., 41, 313–321, doi:10.1080/10256010500384572, 2005.

Ishijima, K., Sugawara, S., Kawamura, K., Hashida, G., Morimoto, S., Murayama, S., Aoki, S., and Nakazawa, T.: Temporal variations of the atmospheric nitrous oxide concentration and its δ^{15}N and δ^{18}O for the latter half of the 20th century reconstructed from firn air analyses, J. Geophys. Res., 112, D03305, doi:10.1029/2006JD007208, 2007.

Miller, B. R., Weiss, R. F., Salameh, P. K., Tanhua, T., Greally, B. R., Mühle, J., and Simmonds, P. G.: Medusa: A sample preconcentration and GC/MS detector system for in situ measurements of atmospheric trace halocarbons, hydrocarbons, and sulfur compounds, Anal. Chem., 80, 1536–1545, doi:10.1021/ac702084k, 2008.

Mohn, J., Forss, A. M., Brühlmann, S., Zeyer, K., Lüscher, R., Emmenegger, L., Novak, P., and Heeb, N.: Time-resolved ammonia measurement in vehicle exhaust, Int. J. Environ. Pollut., 22, 342–356, doi:10.1504/IJEP.2004.005548, 2004.

Mohn, J., Werner, R. A., Buchmann, B., and Emmenegger, L.: High-precision δ^{13}C-CO_2 analysis by FTIR spectroscopy using a novel calibration strategy, J. Mol. Struct., 834, 95–101, doi:10.1016/j.molstruc.2006.09.024, 2007.

Mohn, J., Zeeman, M. J., Werner, R. A., Eugster, W., and Emmenegger, L.: Continuous field measurements of δ^{13}C-CO_2 and trace gases by FTIR spectroscopy, Isot. Environ. Healt. S., 44, 241–251, doi:10.1080/10256010802309731, 2008.

Nakayama, T., Fukuda, H., Kamikawa, T., Sugita, A., Kawasaki, M., Morino, I., and Inoue, G.: Measurements of the $3\nu_3$ band of $^{14}N^{15}N^{16}O$ and $^{15}N^{14}N^{16}O$ using continuous-wave cavity ring-down spectroscopy, Appl. Phys. B, 88, 137–140, doi:10.1007/s00340-007-2653-3, 2007.

Nelson, D. D., McManus, J. B., Herndon, S. C., Zahniser, M. S., Tuzson, B., and Emmenegger, L.: New method for isotopic ratio measurements of atmospheric carbon dioxide using a 4.3 μm pulsed quantum cascade laser, Appl. Phys. B, 90, 301–309, doi:10.1007/s00340-007-2894-1, 2008.

Rahn, T. and Wahlen, M.: A reassessment of the global isotopic budget of atmospheric nitrous oxide, Global Biogeochem. Cy., 14, 537–543, 0886-6236/00/1999GB 900070, 2000.

Ravishankara, A. R., Daniel, J. S., and Portmann, R. W.: Nitrous oxide (N_2O): The dominant ozone-depleting substance emitted in the 21st century, Science, 326, 123–125, doi:10.1126/science.1176985, 2009.

Röckmann, T., Kaiser, J., and Brenninkmeijer, C. A. M.: The isotopic fingerprint of the pre-industrial and the anthropogenic N_2O source, Atmos. Chem. Phys., 3, 315–323, 2003, http://www.atmos-chem-phys.net/3/315/2003/.

Röckmann, T. and Levin, I.: High-precision determination of the changing isotopic composition of atmospheric N_2O from 1990 to 2002, J. Geophys. Res., 110, D21304, doi:10.1029/2005JD006066, 2005.

Rothman, L. S., Jacquemart, D., Barbe, A., Benner, D. C., Birk, M., Brown, L. R., Carleer, M. R., Chackerian, C., Chance, K., Coudert, L. H., Dana, V., Devi, V. M., Flaud, J. M., Gamache, R. R., Goldman, A., Hartmann, J. M., Jucks, K. W., Maki, A. G., Mandin, J. Y., Massie, S. T., Orphal, J., Perrin, A., Rinsland, C. P., Smith, M. A. H., Tennyson, J., Tolchenov, R. N., Toth, R. A., Vander Auwera, J., Varanasi, P., and Wagner, G.: The HITRAN 2004 molecular spectroscopic database, J. Quant. Spectrosc. Ra., 96, 139–204, doi:10.1016/j.jqsrt.2004.10.008, 2005.

Solomon, S., Qin, D., Manning, M., Chen, Z., Marquis, M., Averyt, K. B., Tignor, M., and Miller, H. L.: IPCC, 2007: Climate Change 2007: The Physical Science Basis, Cambridge Univ. Press, Cambridge and New York, 987 pp., 2007.

Toyoda, S. and Yoshida, N.: Determination of nitrogen isotopomers of nitrous oxide on a modified isotope ratio mass spectrometer, Anal. Chem., 71, 4711–4718, doi:10.1021/ac9904563, 1999.

Toyoda, S., Yoshida, N., Urabe, T., Aoki, S., Nakazawa, T., Sugawara, S., and Honda, H.: Fractionation of N_2O isotopomers in the stratosphere, J. Geophys. Res., 106, 7515–7522, 2001.

Toyoda, S., Iwai, H., Koba, K., and Yoshida, N.: Isotopomeric analysis of N_2O dissolved in a river in the Tokyo metropolitan area, Rapid Commun. Mass Sp., 23, 809–821, doi:10.1002/rcm.3945, 2009.

Tuzson, B., Mohn, J., Zeeman, M. J., Werner, R. A., Eugster, W., Zahniser, M. S., Nelson, D. D., McManus, J. B., and Emmenegger, L.: High precision and continuous field measurements of $\delta^{13}C$ and $\delta^{18}O$ in carbon dioxide with a cryogen-free QCLAS, Appl. Phys. B, 92, 451–458, doi:10.1007/s00340-008-3085-4, 2008a.

Tuzson, B., Zeeman, M. J., Zahniser, M. S., and Emmenegger, L.: Quantum cascade laser based spectrometer for in situ stable carbon dioxide isotope measurements, Infrared Phys. Techn., 51, 198–206, doi:10.1016/j.infrared.2007.05.006, 2008b.

Uehara, K., Yamamoto, K., Kikugawa, T., and Yoshida, N.: Isotope analysis of environmental substances by a new laser-spectroscopic method utilizing different pathlengths, Sensor Actuat. B, 74, 173–178, doi:10.1016/S0925-4005(00)00729-2, 2001.

Uehara, K., Yamamoto, K., Kikugawa, T., and Yoshida, N.: Site-selective nitrogen isotopic ratio measurement of nitrous oxide using 2 μm diode lasers, Spectrochim. Acta A, 59, 957–962, doi:10.1016/S1386-1425(02)00260-3, 2003.

VDI: 2449 Part 1 – Prüfkriterien von Meßverfahren – Ermittlung von Verfahrenskenngrößen für die Messung gasförmiger Schadstoffe (Immission), Düsseldorf, 45 pp., 1995.

Wächter, H. and Sigrist, M. W.: Mid-infrared laser spectroscopic determination of isotope ratios of N_2O at trace levels using wavelength modulation and balanced path length detection, Appl. Phys. B, 87, 539–546, doi:10.1007/s00340-007-2576-z, 2007.

Wächter, H., Mohn, J., Tuzson, B., Emmenegger, L., and Sigrist, M. W.: Determination of N_2O isotopomers with quantum cascade laser based absorption spectroscopy, Opt. Express, 16, 9239–9244, doi:10.1364/OE.16.009239, 2008.

Well, R., Flessa, H., Xing, L., Xiaotang, J., and Römheld, V.: Isotopologue ratios of N_2O emitted from microcosms with NH_4^+ fertilized arable soils under conditions favoring nitrification, Soil Biol. Biochem., 40, 2416–2426, doi:10.1016/j.soilbio.2008.06.003, 2008.

Werle, P., Mucke, R., and Slemr, F.: The limits of signal averaging in atmospheric trace-gas monitoring by tunable diode-laser absorption-spectroscopy (TDLAS), Appl. Phys. B, 57, 131–139, doi:10.1007/BF00425997, 1993.

Werner, R. A. and Brand, W. A.: Referencing strategies and techniques in stable isotope ratio analysis, Rapid Commun. Mass Sp., 15, 501–519, doi:10.1002/rcm.258, 2001.

Werner, R. A., Rothe, M., and Brand, W. A.: Extraction of CO_2 from air samples for isotopic analysis and limits to ultra high precision $\delta^{18}O$ determination in CO_2 gas, Rapid Commun. Mass Sp., 15, 2152–2167, doi: 10.1002/rcm.487, 2001.

Yoshida, N. and Toyoda, S.: Constraining the atmospheric N_2O budget from intramolecular site preference in N_2O isotopomers, Nature, 405, 330–334, doi:10.1038/35012558, 2000.

Table 1. Trace gas concentrations and N_2O isotopic composition (δ reference point: medical grade N_2O).

	N_2O [ppm]	$\delta^{15}N^{\alpha}$ [‰]	$\delta^{15}N^{\beta}$ [‰]	CO_2 [ppm]	CH_4 [ppm]	CO [ppb]	O_3 [ppb]	H_2O [ppm]
trace gas recovery[1]	0.39	n.a	n.a	35	2.0	350	–	25
	0.35	n.a.	n.a.	–	–	–	–	–
	0.90	n.a.	n.a.	–	–	–	–	–
	9.0	n.a.	n.a.	–	–	–	–	–
isotopic fractionation[2]	0.35	+25.4	+25.4	–	–	–	–	–
	0.90	+25.4	+25.4	–	–	–	–	–
	9.0	+25.4	+25.4	–	–	–	–	–
spectral interference[3]	0.35	n.a.	n.a.	400	2.0	200–450	62–65	1–2%

n.a.: not analyzed

[1] gas mixtures prepared from 9 or 90 ppm N_2O reference gas and synthetic air; line 1: additionally with pressurized air and concentrations determined by FTIR.

[2] gas mixtures prepared from a 90.8 ppm N_2O reference gas with known isotopic composition and synthetic air.

[3] ambient air; N_2O and CO_2 concentrations based on estimates, all other concentrations taken from routine measurements of the Swiss National Air Pollution Monitoring Network (NABEL).

AMTD
2, 3099–3127, 2009

Table 2. High-precision recovery of N_2O after preconcentration (n=3). Error bars represent the expanded uncertainty (95% confidence level).

N_2O input concentration	Recovery [%]
350 ppb	100.1±0.1
900 ppb	100.2±0.4
9.0 ppm	100.0±0.1

Table 3. Changes in the N_2O isotopomer ratios ($\Delta\delta^{15}N=\delta^{15}N_{precon}-\delta^{15}N_{original}$) after dilution and preconcentration compared to the unprocessed calibration gas (n=3–5). Error bars represent the expanded uncertainty (95% confidence level).

N_2O input concentration	$\Delta\delta^{15}N^{\alpha}$ [‰]	$\Delta\delta^{15}N^{\beta}$ [‰]
350 ppb	0.06±0.31	0.34±0.52
900 ppb	0.08±0.42	0.19±0.40
9.0 ppm	−0.05±0.38	0.07±0.80

AMTD
2, 3099–3127, 2009

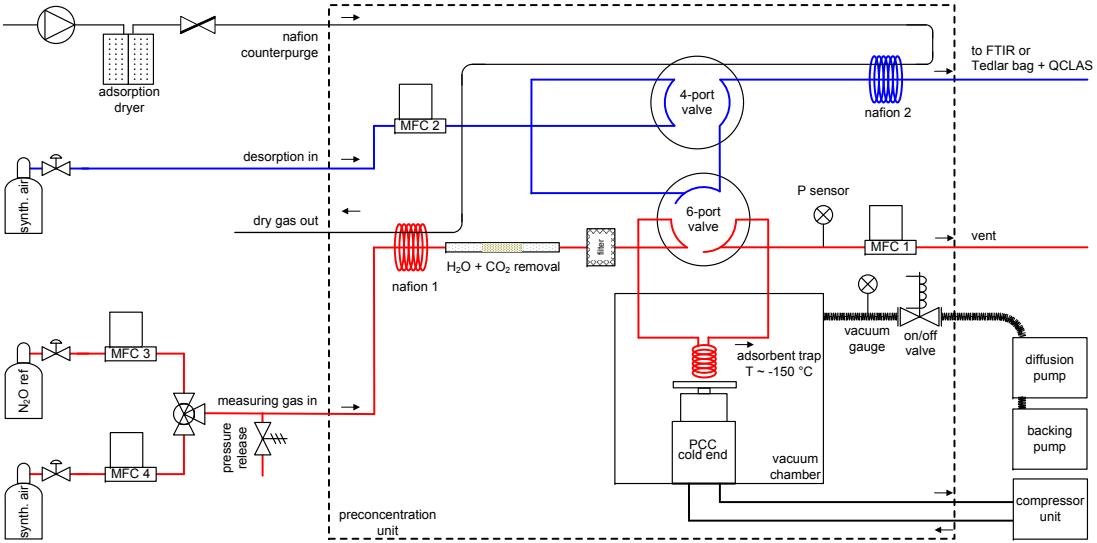

Fig. 1. Process chart during trap loading (phase II) with N_2O in synthetic air.

AMTD
2, 3099–3127, 2009

Liquid nitrogen-free preconcentration unit

J. Mohn et al.

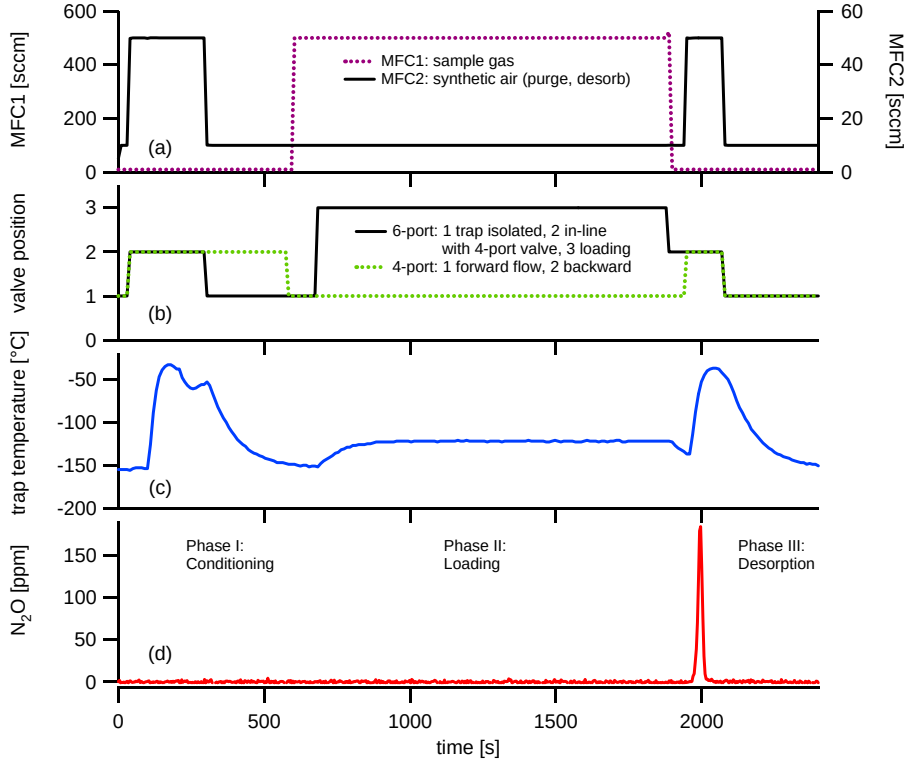

Fig. 2. Typical N_2O adsorption/desorption process (adsorption of 500 sccm of 350 ppb N_2O in synthetic air; 10 l sample volume) with preceding trap conditioning: **(a)** sample gas flow (MFC1) and flow of synthetic air (MFC2); **(b)** position of 6-port and 4-port valves; **(c)** trap temperature; **(d)** N_2O concentration profile as analyzed by on-line FTIR spectroscopy.

AMTD
2, 3099–3127, 2009

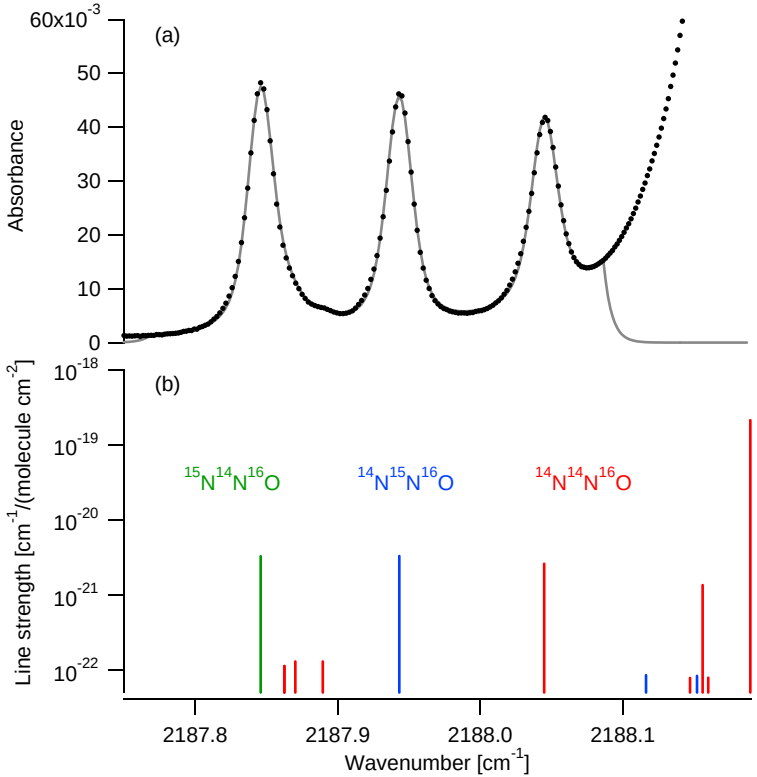

Fig. 3. **(a)** Measured (dots) and fitted spectrum (solid line) of the N_2O isotopes at 90 ppm and **(b)** the corresponding line strengths. The tail of a strong absorption line of $^{14}N^{14}N^{16}O$ (2188.19 cm^{-1}) is clearly visible and was considered in the fit up to 2188.1 cm^{-1}.

AMTD
2, 3099–3127, 2009

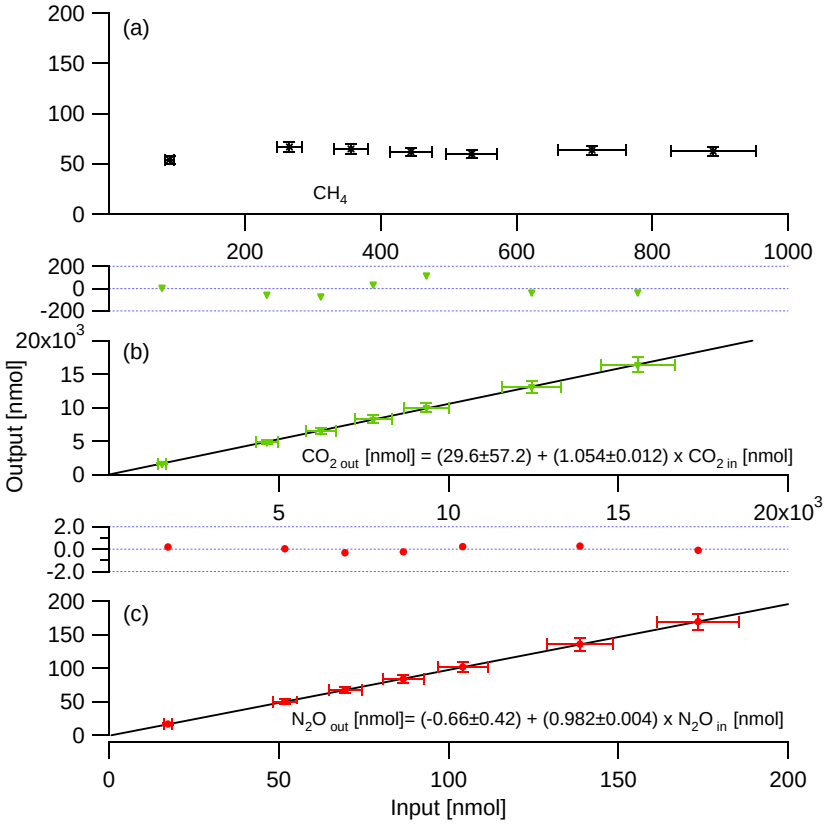

Fig. 4. Amount of **(a)** CH_4, **(b)** CO_2, and **(c)** N_2O concentrated on the HayeSep D trap depending on the sample volume from 1 to 10 l (adsorption: 100 sccm of 390 ppb N_2O, 35 ppm CO_2, 2.0 ppm CH_4, 350 ppb CO, 25 ppm H_2O in 80% N_2 and 20% O_2). Error bars represent the expanded standard uncertainty. For CO_2 and N_2O deviations from linearity are given in nmol.

AMTD
2, 3099–3127, 2009

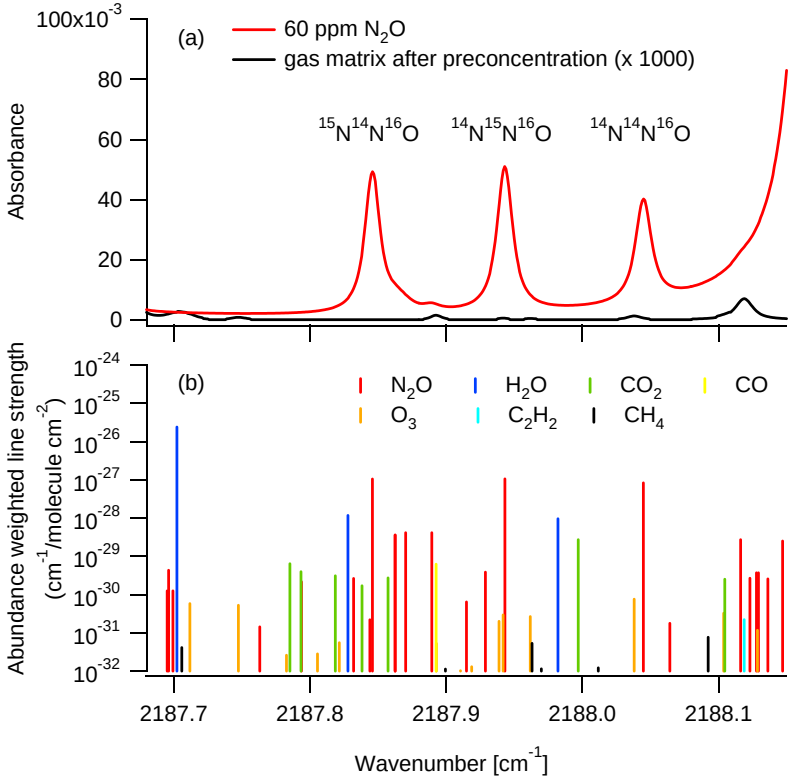

Fig. 5. **(a)** Simulated absorption spectra of N_2O and preconcentrated ambient air (magnified by a factor 1000). **(b)** Absorption lines of atmospheric constituents in the wavelength region selected for N_2O isotopomer analysis.

AMTD
2, 3099–3127, 2009